The Joint Effects of Nitriding and Parameters Related to the Destabilisation of Austenite on Wear Resistance in White Cast Iron with 25% Cr

Alejandro González-Pociño [ID], Florentino Alvarez-Antolin *[ID] and Juan Asensio-Lozano [ID]

Materials Pro Group, Departamento de Ciencia de los Materiales e Ingeniería Metalúrgica, Universidad de Oviedo, Independencia 13, 33004 Oviedo, Spain; gonzalezpalejandro@uniovi.es (A.G.-P.); jasensio@uniovi.es (J.A.-L.)
* Correspondence: alvarezflorentino@uniovi.es; Tel.: +34-985-181-949

Abstract: In this article, the effects of an ionic nitriding treatment are analysed, together with deliberate variation of different thermal parameters associated with the destabilisation of austenite, on erosive wear resistance of white cast irons with 25% Cr. The methodology followed in this research was an experimental design, where six factors were analyzed by performing eight experiments. The thickness of the nitrided layer is much smaller than in white cast iron with lower percentages in Cr, never reaching 20 microns. The nitriding treatment entails considerable softening of the material underneath the nitriding layer. This softening behaviour becomes partially inhibited when the destabilisation temperature of austenite is 1100 °C and dwell times at such temperature are prolonged. This temperature seems to play a significant role in the solubilization of non-equilibrium eutectic carbides, formed during industrial solidification. The nitriding treatment leads to additional hardening, which, in these cases, favours a second destabilisation of austenite, with additional precipitation of secondary carbides and the transformation of retained austenite into martensite. Despite softening of the material, the nitriding treatment, together with air-cooling after destabilisation of the austenite, allows a noticeable increase in resistance to erosive wear.

Keywords: erosive wear resistance; white cast irons containing 25% Cr; nitriding; destabilization of austenite; secondary carbides

1. Introduction

White cast irons highly alloyed with chromium have been widely used in very aggressive settings where a high level of resistance to erosive and abrasive wear is required. This high resistance is attributed to the presence of eutectic carbides of the type M_7C_3 [1,2]. The hardness of these carbides can be found in the range of 1200 HV [1]. At the same time, these carbides are found embedded in a matrix of hard martensite and retained austenite, which lends the material a greater tenacity than traditional Nihard cast irons [1]. The Cr dissolved in the matrix constituent also favours resistance to erosive wear and resistance to oxidation [2]. To improve resistance to wear, it is recommendable to carry out a destabilisation treatment of the austenite [3–5]. Austenite is found in a very alloyed state, which creates difficulties in the spread of C and, so, the times required for this destabilisation are long. During destabilisation of austenite the precipitation of secondary carbides is produced, which has a positive effect on resistance to wear [5–11]. At the same time, the Ms temperature rises, thus reducing the percentage of retained austenite [12]. If the time of permanence at the destabilisation temperature is high, dissolution of those eutectic carbides precipitated may be produced simultaneously as a consequence of non-equilibrium solidification [6,13]. All of these factors could have a very significant influence on the in-service behaviour of these alloys. White cast irons with 25% chromium show a high resistance to wear. In these white cast irons, the microstructure of the matrix constituent is very

significant with regard to resistance to wear. This microstructure basically depends on the temperature of tempering. Tempering at 500 °C and tempering times of around 6 h favour an increase in wear resistance, since, under these tempering conditions, the presence of retained austenite is eliminated and the percentage of secondary carbides of the type M_7C_3 is increased [13,14]. An additional nitriding treatment could produce superficial hardening and favour an increase in resistance to erosive wear by the formation of sub-nitrides in the tempered martensite matrix. The presence of Cr, as the main alloying element in these alloys, could favour an additional hardening through a nitriding treatment [15]. This hardening could favour greater resistance to wear. However, this treatment is carried out at temperatures of around 500 °C [15], which could mean a softening of the surface areas of the material, which are not affected by the nitriding. The presence of tempered martensite would favour the diffusion of N [16], since N diffuses through of octahedral interstitial sites of the Fe-BCC [17]. The nitride layer could be made up of nitrides of the type ε-$Fe_{2\text{-}3}N$ and of the type γ'-Fe_4N [17], which generate elevated distortion in the ferritic matrix. The thickness of this nitrided layer in white cast irons with 18% Cr is around 60–70 microns [10]. At the same time, nitriding favours the transformation of carbides M_7C_3 into carbonitrides [18,19]. In this study, by means of the application of an experimental design, an analysis is made of the joint effect of the variation of different thermal parameters associated with the destabilisation of austenite and the application of a plasma nitriding treatment on the resistance and wear of white cast irons with 25% Cr. Erosive wear is a phenomenon of surface damage that is caused by the impact of solid particles [2]. This type of wear, in the processing of this alloy, combines mechanisms of wear by impact and mechanisms of abrasive wear [20,21]. Erosion due to impact of hard particles is a common problem during crushing/grinding operations [22]. This study comes about as a complement and continuation of a previous study carried out by the authors on this same question [7]. This analysis includes the effect of the nitriding treatment (temperatures of 500 °C) on the part of the material not affected by nitriding.

2. Materials and Methods

Table 1 shows the chemical composition of the white cast iron analysed. The material used in this research was supplied by the Spanish company, Fundiciones del Estanda, S.A. (Beasain, Spain), and the chemical composition is that which is indicated by this company. The research methodology followed was the application of a fractional experimental design, where six factors were analysed by carrying out eight experiments [23].

Table 1. Chemical composition (% weight).

C	Si	Mn	Cr	Mo
2.7	1.2	0.8	25.1	0.5

Table 2 shows the analysed factors and the levels of analysis in each of these factors. It should be highlighted, with reference to factor B, that the experimental permanence times at the destabilisation temperature of austenite, were higher than usual. In view of this, the intention was to analyse the influence of a possible re-dissolution of carbides, precipitated as a consequence of non-equilibrium solidification, whose kinetics are complementary to that of secondary carbide precipitation of the type M_7C_3 during destabilisation of austenite.

In this study, the effect of six factors in eight experiments has been analysed. This entails a loss of information, corresponding to the majority of interactions. In order to be able to analyse all possible interactions 64 ($2^6 = 64$) experiments would need to be carried out. However, in this case, only eight effects (2^{6-3}) have been considered, which means a high loss of information which, however, is not significant in industrial practice. Table 3 shows the matrix of experiments. Columns D, E and F have been constructed from the product of columns A × B, A × C, and B × C. The column 'confounding patterns' shows the main effects and interactions of 2 factors whose effects remain confounded with the main effects.

Table 2. Factors and levels.

Factors		Levels	
Code	Thermal Parameter	Level −1	Level +1
A	Temperature of destabilisation of the austenite (°C)	1000	1100
B	Time of permanence at the destabilisation temperature (h)	4	8
C	Nitriding	no	yes
D	Means of cooling in tempering	air	oil
E	Temperature of tempering (°C)	200	500
F	Time of permanence in tempering (h)	3	6

Table 3. Matrix of experiments.

Experiment	A	B	C	D	E	F	Confounding Patterns
1	−1	−1	−1	+1	+1	+1	
2	+1	−1	−1	−1	−1	+1	A + BD + CE
3	−1	+1	−1	−1	+1	−1	B + AD + CF
4	+1	+1	−1	+1	−1	−1	C + AE + BF
5	−1	−1	+1	+1	−1	−1	D + AB + EF
6	+1	−1	+1	−1	+1	−1	E + AC + DF
7	−1	+1	+1	−1	−1	+1	F + BC + DE
8	+1	+1	+1	+1	+1	+1	AF + BE + CD

Table 4 shows the main process parameters with which nitriding was carried out in experiments 5 to 8.

Table 4. Parameters used in the plasma nitriding process.

Gas Mixture	$70\%N_2 + 30\%H_2$
Gas flux (cm^3/min)	500
Temperature (°C)	540
Pressure (Pa)	400
Time (min)	120
Output voltage (V)	500

The results analysed were the resistance to erosive wear and the hardness of the material in the area adjacent to the nitrided layer. The test of resistance to erosive wear was carried out according to norm ASTM G76, by means of compressed air blasting with corundum particles. These corundum particles had a size of 50 µm. The pressure applied was 2 bar, and the flow of corundum was 100 g/min. The angle of incidence on the surfaces of the samples was 30°. The time used in each experiment was 4 minutes. Three repetitions per test were carried out.

Given that, the nitriding treatment entails maintaining the material at 540 °C for 2 h, the area not affected by the diffusion of N could be exposed to a kind of second tempering. This could affect the resistance of the material to wear, once the signs of wear pass through the nitrided layer. To analyse the influence of the nitriding treatment on the interior area, adjacent to the nitrided layer, tests were carried out on hardness and micro-hardness at an approximate distance of 2 mm from the end of the nitrided layer. Tests of micro-hardness were carried out with localised indentations in the constituent matrix. The load applied in hardness tests was of 300 N and in tests of micro-hardness, it was of 0.5 N.

The statistical analysis was carried out with the help of the programme Statgraphics Centurion XVI, version 16.1.18 (Statgraphics Technologies, Inc., The Plains, VA, USA).

For metallographic inspection, the samples were cut further and bakelite was mounted, followed by mechanical grinding with SiC sandpaper of 240, 320, 400, and 600 grit. Textile cloths with 6 and 1 micron diamond paste were used during the mechanical polishing. For final observation, the samples were further etched with nital 4 (4 mL nitric acid and

96 mL ethanol). The microstructures of the samples were analyzed under a NIKON Epiphot 200 optical microscope. The scanning electron microscope employed was a JEOL JSM-5600 (Japan Electron Optics Laboratory, Tokyo, Japan), equipped with the characteristic energy dispersive X-ray (EDX) microanalysis system.

The phases present on the nitrided surface were determined by X-ray diffraction on a XRD 3000 T/T diffractometer (SEIFERT, Baker Hughes, Celle, Germany). The radiation was emitted via a fine-focus Mo tube at a working power of 40 kV $\times$ 40 mA and monochromatized to the Kα doublet: λ_1 = 0.7093616 Å and λ_2 = 0.713607 Å. The diffracted intensity was determined in a 2θ range from 7 to 38°, with an angular step and counting time of approximately 0.03° and 22 s, respectively

3. Results

Figure 1 shows the initial microstructure, corresponding to the as-cast state. This microstructure is made up of proeutectic austenite, with mainly dendritic growth, see Figure 1a. At the same time, an eutectic constituent can be seen, formed mainly by austenite and mixed carbides of Fe and Cr with stoichiometry M_7C_3, see Figure 1b,c. In Figure 1d the presence of a high density of secondary mixed carbides can be observed in the interior of the austenite grain. Table 5 shows a semi-quantitative analysis of these carbides. All these carbides seem to be of the type M_7C_3 and $M_{23}C_6$. Two groups of carbides can be distinguished. The smallest and brightest (spectrums 2, 3 and 4) are those which present a lower Cr content. These carbides could be associated with mixed carbides of stoichiometry $M_{23}C_6$ Those which are a little bigger, with a slightly darker colouring, present a greater quantity of chrome (spectrum 5). These carbides could be associated with mixed carbides of stoichiometry M_7C_3. The latter have more similarity to eutectic carbides (spectrum 1). Both types of carbides, with a greater content of Cr, also contain Mo (spectrums 1 and 5). Figure 1e shows the presence of eutectic carbides that could be associated with mixed carbides of stoichiometry M_2C, associated with the Mo. These carbides show a more elongated and narrow morphology than the previous carbides. Due to the high hardenability of these cast irons, the austenite will be transformed into martensite by simple air cooling. This slow cooling favours the presence of retained austenite after hardening. High tempering, at around 500 °C, could favour a second destabilisation of the austenite and its later transformation into martensite after cooling [15].

Table 5. Semi-quantitative analysis of the carbides highlighted in Figure 1. This analysis was carried out through an energy dispersive X-ray microanalysis (EDX). (% atomic).

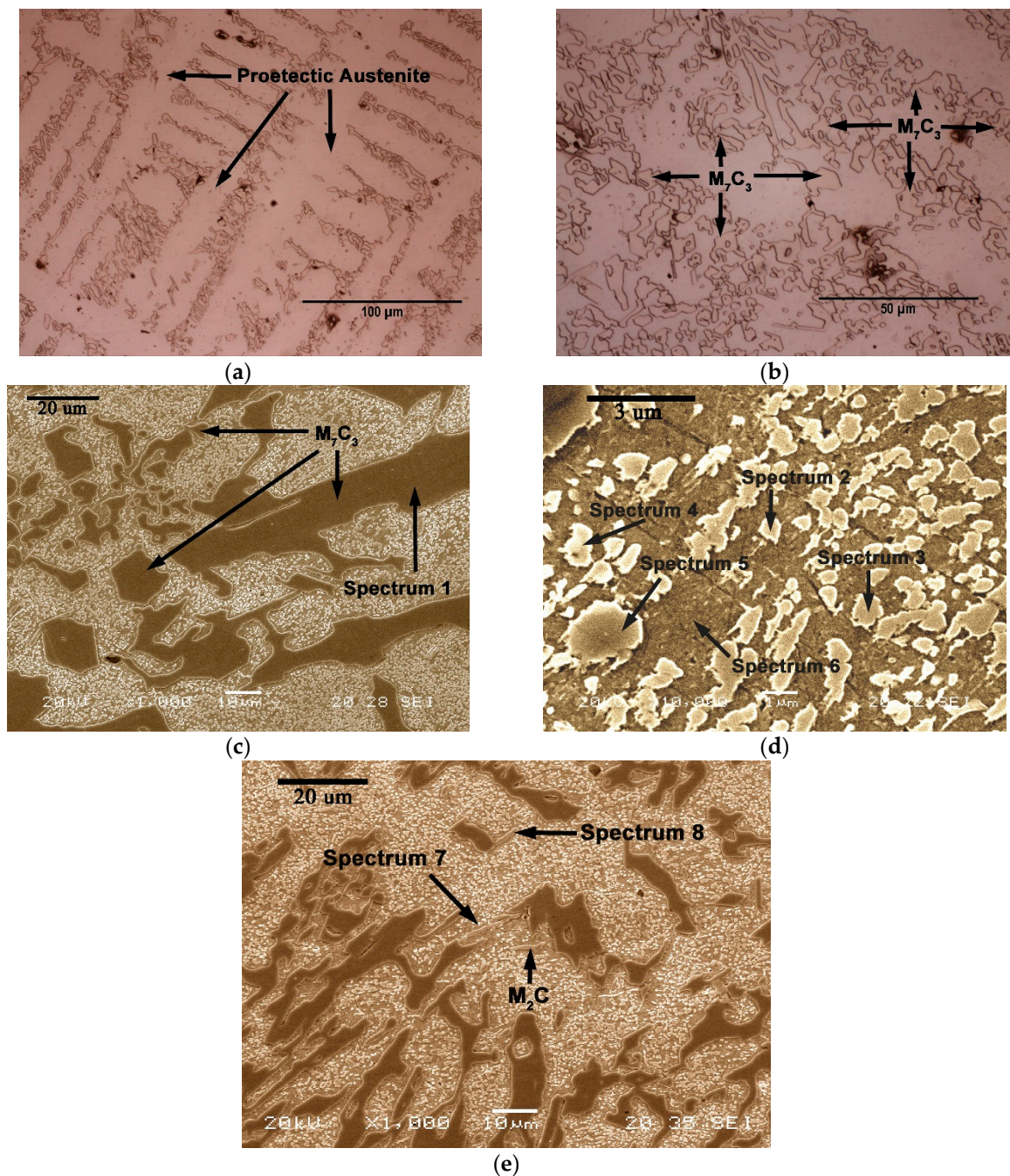| Spectrum	C	Cr	Fe	Mo	Si
1	38	38	23	0.8	-
2	30	9	61	-	-
3	40	9	51	-	-
4	33	7	60	-	-
5	36	37	26	0.7	-
6	27	6	67	0.2	2
7	26	10	48	16	-
8	28	9	47	16	-

Figure 1. Microstructure as-cast. (**a**) The dendritic growth of pro-eutectic austenite can be seen. Micrograph obtained by optical microscope (magnification of 500×); (**b**) eutectic carbides M_7C_3 can be seen. Micrograph obtained by optical microscope (magnification of 1000×); (**c**) eutectic carbides of the type M_7C_3 can be seen. Micrograph obtained by scanning electron microscope (magnification of 1000×); (**d**) presence of secondary carbides of the type M_7C_3 and $M_{23}C_6$. Micrographic obtained by scanning electron microscopy (magnification of 10,000×); (**e**) presence of mixed eutectic carbides of the type M_2C, associated with the Mo (magnification of 1000×).

Table 6 shows the results obtained from the wear test. Figure 2 shows the representation of the effects in a normal probability plot, highlighting those that present a significant effect on resistance to erosive wear. The C factors (nitriding) and D factors (through cooling during tempering) show a significant effect, in such a way that if factor C is situated at level −1 (without nitriding) and D at level +1 (tempered in oil), an increase in wear is produced, that is to say, these conditions would be those which offer lower resistance to erosive wear. In previous research, it was concluded that through air-cooling in tempering

a greater precipitation of secondary carbides of the type M_7C_3 is produced than if cooling is carried out in oil. This is due to the fact that slower cooling speeds favour the kinetics of precipitation by nucleation and growth of carbides in the interval of temperatures between 600 °C and 400 °C [6]. Also, the significant effect of the interactions of second grade AF + BE + CD can be observed. These interactions are analysed in Figure 3. It can be seen that the interaction which has a more significant effect is CD, given that when factor C is situated at level +1 (with nitriding) and D at level −1 (air cooling), is when the least wear is produced.
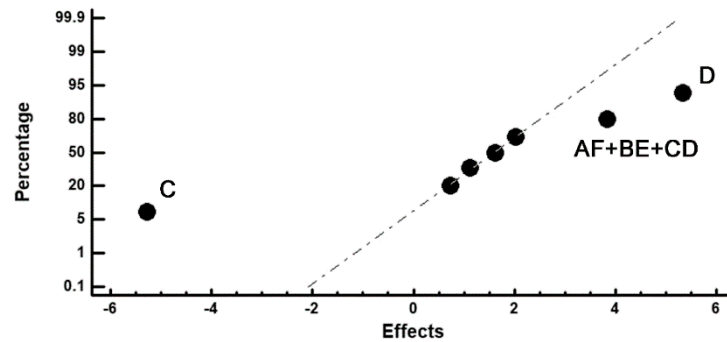

Figure 2. Representation of the effects on a normal probability plot. Those factors with a significant effect on resistance to erosive wear are highlighted.
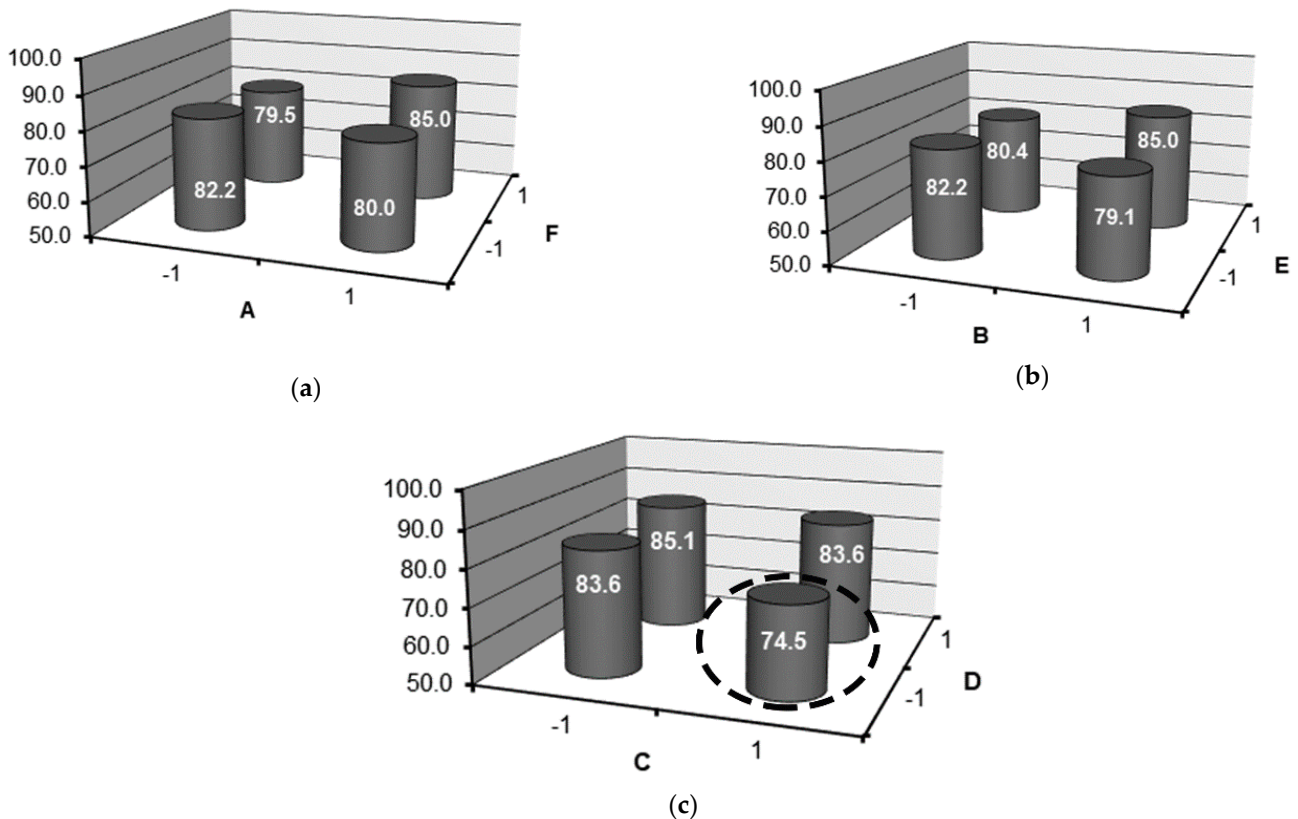

(**a**)

(**b**)

(**c**)

Figure 3. Analysis of the interactions AF + BE + CD. (**a**) interaction AF; (**b**) interaction BE; (**c**) interaction CD.

Table 6. Weight loss in the erosive wear (mg) test. The effects refer to the confounding pattern highlighted in the right-hand column. The average values refer to the average value of the 8 experiments.

Experiment	Erosive Wear		Confounding Pattern
	mg	Effect	
1	85.5	81.712	Average
2	83.6	1.62	A + BD + CE
3	83.6	0.72	B + AD + CF
4	84.7	−5.27	C + AE + BF
5	80.9	5.32	D + AB + EF
6	75.4	2.02	E + AC + DF
7	73.6	1.12	F + BC + DE
8	86.4	3.82	AF + BE + CD

Figure 4 shows an example of the morphology of signs of wear. Figure 4a–c shows the morphology of the signs of wear corresponding to experiment 1, and Figure 4d–f shows the morphology of the signs of wear corresponding to experiment 7. In all of the 8 experiments, the depth of profile of the signs of wear never reached more than 2.2 mm.

In all of those samples subjected to a nitriding treatment, experiments 5 to 8, the thickness of the nitride layer was very small, never reaching 20 microns and resulting in an average thickness of less than 10 microns in all cases. Figure 5a shows an example of the thickness of the nitride layer, in this case corresponding to experiments 5. Figure 5b–d highlight areas, which were analysed through an energy dispersive X-ray microanalysis (EDX). The EDX analysis was performed on metallographic samples in the polished state, without etching with a chemical reagent. Table 7 shows the results obtained. It should be pointed out that the eutectic carbides of the type M_7C_3 included in the thickness of the nitrided layer were not affected by N (spectrums 1,4 and 6). However, the constituent matrix presents increasing quantities of N from the interior of the layer to its outer edge. See spectra 2, 3 and 6. It must be pointed out that the greater part of the nitrogen is concentrated on the extreme outer edge of the nitride layer, which entails only a few microns (see the "mapping" of elements in Figure 5b).

Table 7. Semi-quantitative analysis of phases shown in Figure 5b. This analysis was carried out through an energy dispersive X-ray microanalysis (EDX). (% atomic).

Spectrum	C	N	Cr	Fe
1	32	–	49	19
2	26	2	14	58
3	30	10	42	18
4	32	–	48	20
5	32	30	18	20
6	32	–	50	18

Figure 6 shows the diffractogram obtained on the surface of the sample corresponding to experiment 8, showing the main phases identified. It must be highlighted that the presence of CrN and Fe_4N has been detected. These precipitates are so fine that they are not detected by SEM. The presence of fine carbides of the M_3C type, precipitated during the tempering of the martensite, has also been detected.
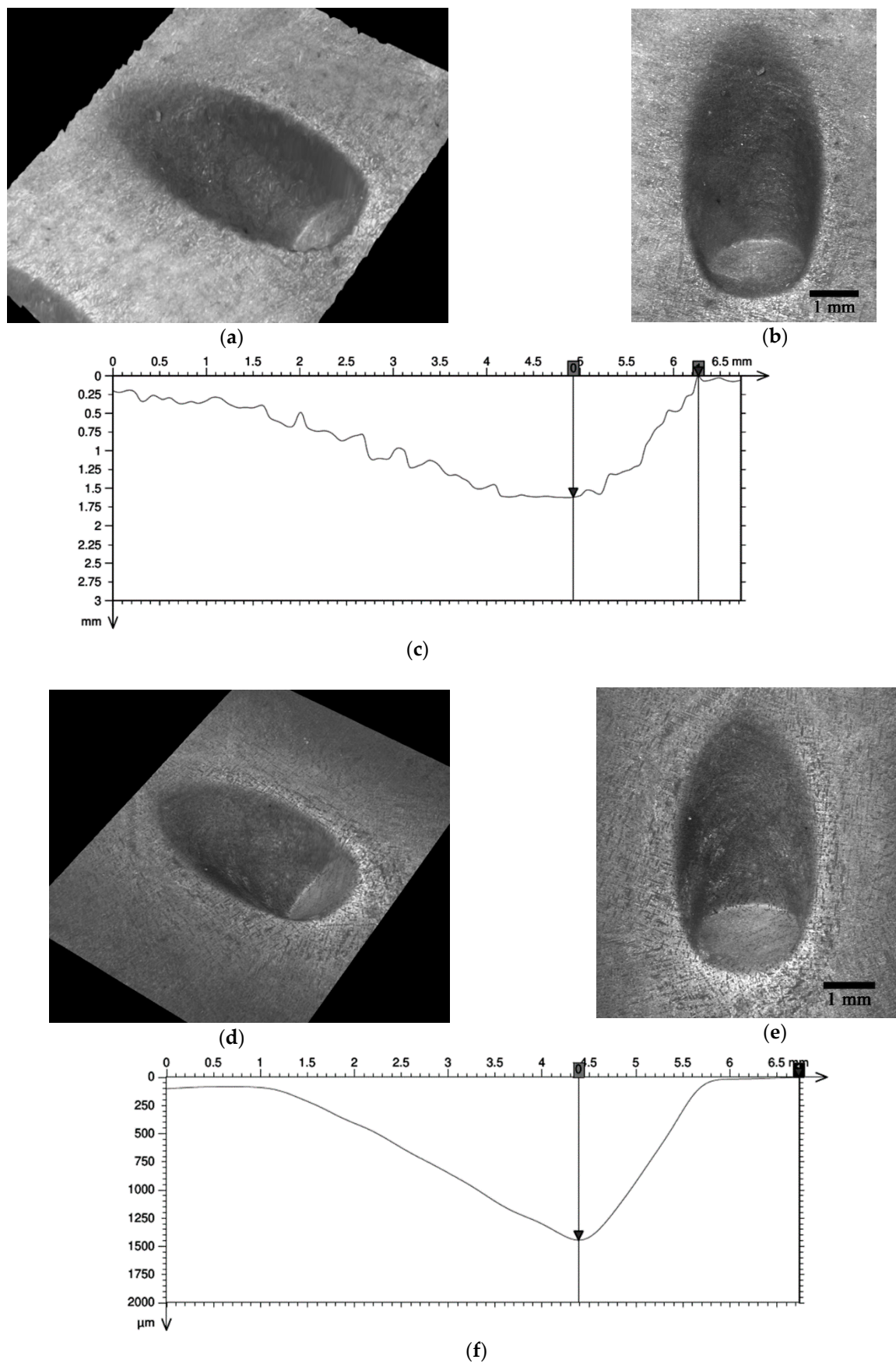
Figure 4. Morphology of the signs of erosive wear. (**a**–**c**) corresponding to experiment 1; (**d**–**f**) corresponding to experiment 7.
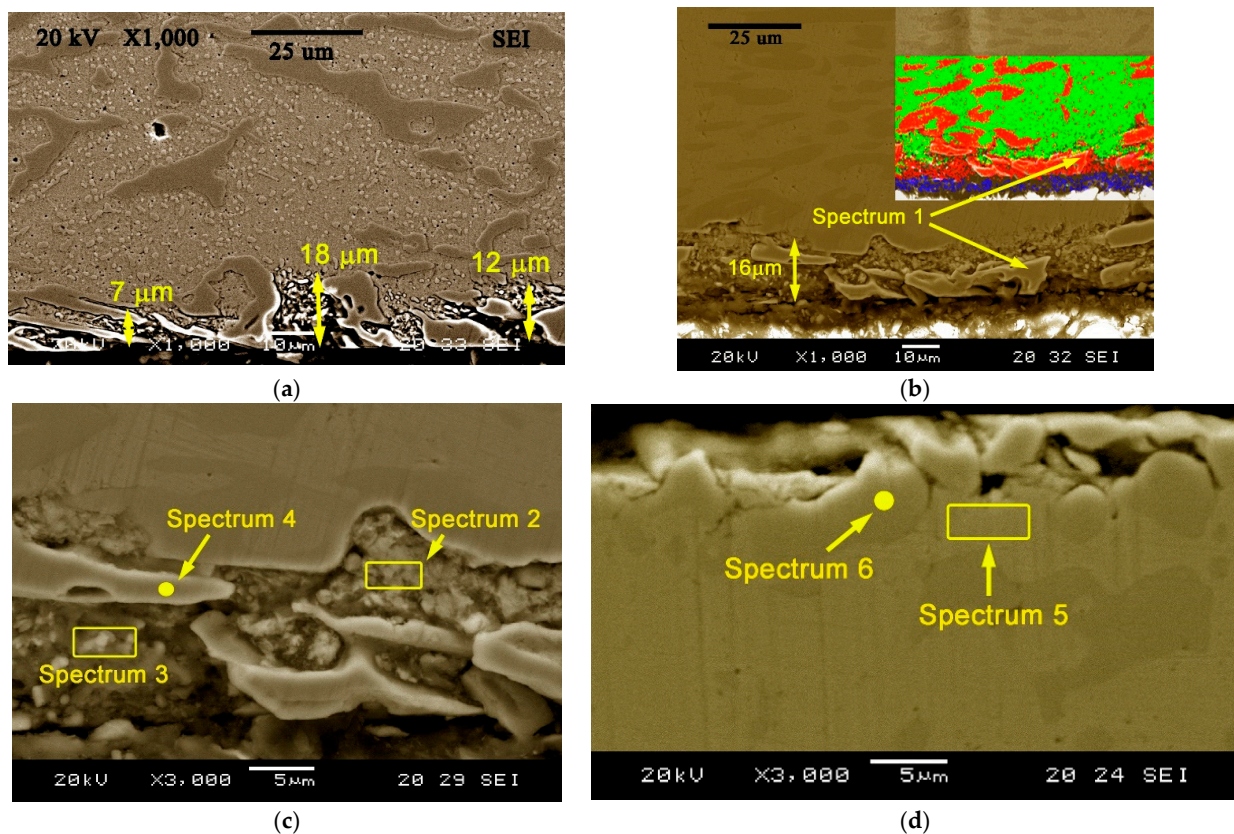
(a)

(b)

(c)

(d)

Figure 5. Thickness of the nitrided layer (SEM). (**a**) Experiment 5. Magnification of 1000×; (**b**) Mapping of elements by means of energy dispersive X-ray (EDX) microanalysis, corresponding to experiment 5. Blue: N; Red: Cr; Green Fe. Magnification of 1000×; (**c**) EDX analysis of the nitrided layer corresponding to experiment 7. Magnification of 3000×; (**b**) EDX analysis of the nitrided layer corresponding to experiment 8. Magnification of 3000×.
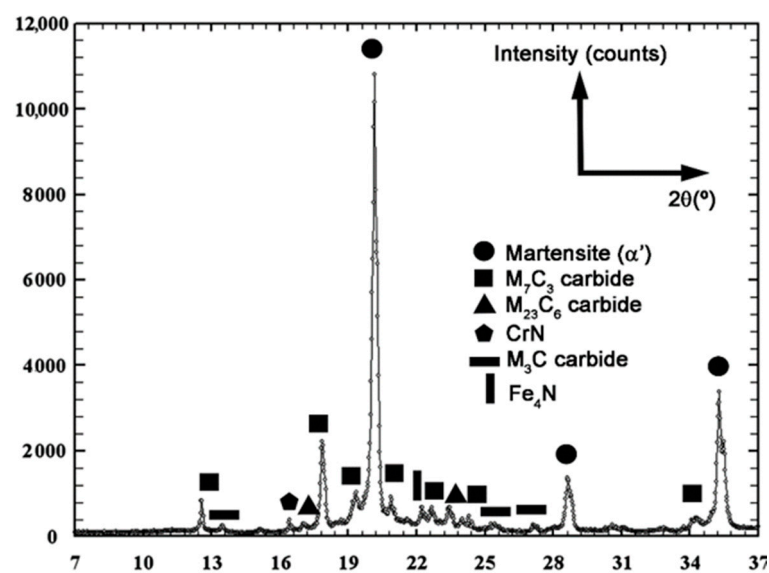

Figure 6. Diffractogram of the nitrided surface of sample corresponding to experiment 8.

Table 8. shows the results of the average values obtained on the hardness of the inside area adjacent to the nitride layer. At the same time, it shows the results of the effects, referring to the confounding pattern that is shown in the matrix of the experiments.

Figure 7a shows the representation of the effects on a normal probability plot, highlighting those that present a significant effect on overall hardness, and Figure 7b shows the

representation of the effects on a normal probability plot, highlighting those that present a significant effect on hardness in the constituent matrix (micro-hardness). In both cases, factor C (nitriding) has a significant effect on hardening, in such a way that, if this factor is situated in its level-1 (without nitriding), an increase is produced in the overall hardness and the constituent matrix. So, nitriding treatment entails great softening of the alloy in inside areas adjacent to the nitrided layer. It must also be pointed out that factors A and B (A= destabilisation temperature of austenite and B= time of permanence at the destabilisation temperature) have a significant effect on both hardnesses. From this, nitriding treatment has a less negative effect on hardness in the interior of the nitrided layer when the destabilisation treatment of austenite is carried out at 1100 °C, for prolonged periods of time, around 8 hours. In a preliminary study, it was confirmed that in these conditions, greater dissolution was produced of those primary carbides that precipitated as a consequence of a non-balanced solidification, thus increasing the content of C dissolved in the austenite. This means that, after quenching, the microstructure showed a greater quantity of retained austenite. Through tempering at 500 °C a second destabilisation of austenite was produced, with the precipitation of new secondary carbides and the transformation of this austenite into martensite [7]. This appears to reduce the 'softening' of the material during the nitriding treatment.
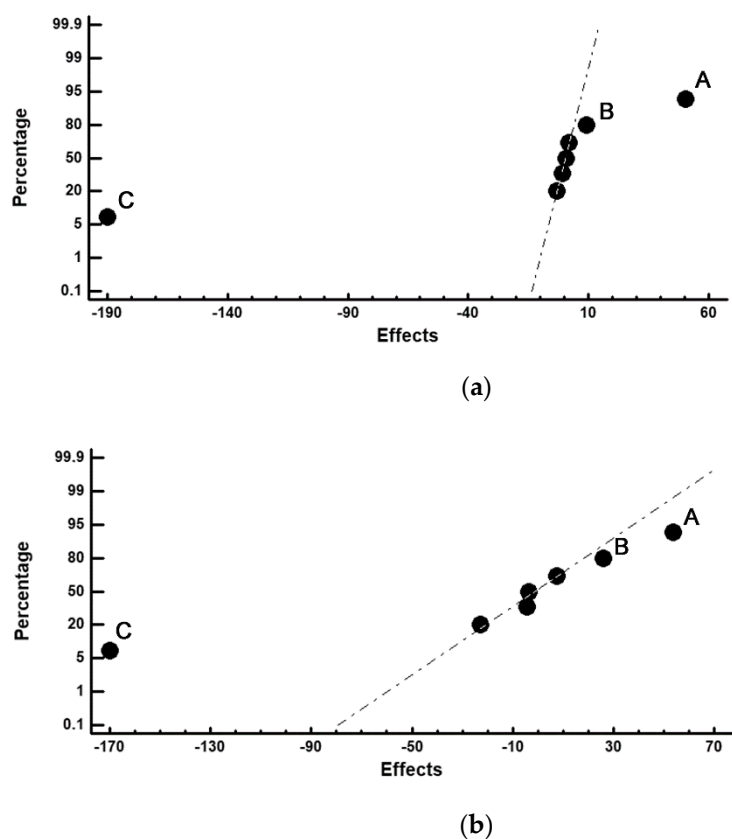

(**a**)

(**b**)

Figure 7. Representation of the effects on a normal probability plot. Those factors are highlighted which have a significant effect on hardness at an approximate distance of 2 mm from the termination of the nitrided layer. (**a**) Vickers hardness with a load of 300 N; (**b**) Vickers hardness with a load of 0.5 N applied to the constituent matrix.

Table 8. Average hardness measures to an interior distance of 2 mm from the end of the nitride layer.

Experiment	Hardness (HV)		Micro-Hardness (HV)		Confounding Pattern
	F = 10 N	Effect	F = 0.5 N	Effect	
1	699	633.87	645	619.00	Average
2	746	50.2	714	53.5	A + BD + CE
3	710	9.2	706	26.0	B + AD + CF
4	760	−189.7	751	−170.0	C + AE + BF
5	510	0.75	509	−4.5	D + AB + EF
6	562	1.75	556	−3.5	E + AC + DF
7	516	−3.25	509	−23.0	F + BC + DE
8	568	−0.75	562	7.5	AF + BE + CD

4. Conclusions

In this study, through the application of an experimental design, the joint effects are analysed of an ionic nitriding treatment and the variation of different thermal parameters associated with the destabilisation of austenite, on the resistance to wear of white cast irons with 25% Cr. The main conclusions are the following:

1. The thickness of the nitrided layer is much smaller in white cast irons with lower percentages of Cr, not reaching 20 microns in any of the experiments carried out. N has been detected forming very fine nitrides of the type CrN and Fe_4N.
2. The nitriding treatment entailed a considerable softening of the material, once the nitrided layer was passed. This softening is 'reduced' when the temperature of destabilisation of the austenite is at 1100 °C. This temperature accelerates the dissolution of eutectic carbides, precipitated as a consequence of non-equilibrium solidification. The nitriding treatment entails an additional tempering which favours a second destabilisation of the austenite with an additional precipitation of secondary carbides and the transformation of the possible retained austenite into martensite.
3. Despite this, the nitriding treatment, together with air-cooling, after the destabilisation of austenite, allows a considerable increase in resistance to erosive wear.

Author Contributions: J.A.-L. Conceived and designed the investigation; A.G.-P. Performed all laboratory work; F.A.-A. Led the investigation, analysed the data and wrote the paper. All authors have read and agreed to the published version of the manuscript.

Institutional Review Board Statement: Not applicable.

Informed Consent Statement: Not applicable.

Data Availability Statement: Data is contained within the article.

Conflicts of Interest: The authors declare no conflict of interest.

References

1. Chung, R.J.; Tang, X.; Li, D.Y.; Hinckley, B.; Dolman, K. Effects of titanium addition on microstructure and wear resistance of hypereutectic high chromium cast iron Fe-25wt.%Cr-4wt.%C. *Wear* **2009**, *267*, 356–361. [CrossRef]
2. Zhang, Y.; Shimizu, K.; Yaer, X.; Kusumoto, K.; Efremenko, V.G. Erosive wear performance of heat treated multi-component cast iron containing Cr, V, Mn and Ni eroded by alumina spheres at elevated temperatures. *Wear* **2017**, *390–391*, 135–145. [CrossRef]
3. Guitar, M.A.; Suarez, S.; Prat, O.; Guigou, M.D.; Gari, V.; Pereira, G.; Mucklich, F. High Chromium Cast Irons: Destabilized-Subcritical Secondary Carbide Precipitation and Its Effect on Hardness and Wear Properties. *J. Mater. Eng. Perform.* **2018**, *27*, 3877–3885. [CrossRef]
4. Karantzalis, A.E.; Lekatou, A.; Diavati, E. Effect of Destabilization Heat Treatments on the Microstructure of High-Chromium Cast Iron: A Microscopy Examination Approach. *J. Mater. Eng. Perform.* **2009**, *18*, 1078–1085. [CrossRef]
5. Gasan, H.; Erturk, F. Effects of a Destabilization Heat Treatment on the Microstructure and Abrasive Wear Behavior of High-Chromium White Cast Iron Investigated Using Different Characterization Techniques. *Metall. Mater. Trans. A Phys. Metall. Mater. Sci.* **2013**, *44A*, 4993–5005. [CrossRef]
6. Gonzalez-Pociño, A.; Alvarez-Antolin, F.; Asensio-Lozano, J. Erosive Wear Resistance Regarding Diferent Destabilization Heat Treatments of Austenite in High Chromium White Cast Iron, Alloyed with Mo. *Metals* **2019**, *9*, 522. [CrossRef]

7.   Gonzalez-Pocino, A.; Alvarez-Antolin, F.; Asensio-Lozano, J. Optimization of Thermal Processes Applied to Hypoeutectic White Cast Iron containing 25% Cr Aimed at Increasing Erosive Wear Resistance. *Metals* **2020**, *10*, 359. [CrossRef]
8.   Ortega-Cubillos, P.; Nannetti-Bernardini, P.A.; Celso-Fredel, M.; Antonio Campos, R. Wear resistance of high chromium white cast iron for coal grinding rolls. *Revista Facultad de Ingeniería* **2015**, *0*, 134–142. [CrossRef]
9.   Bedolla-Jacuinde, A.; Guerra, F.V.; Mejia, I.; Zuno-Silva, J.; Rainforth, M. Abrasive wear of V-Nb-Ti alloyed high-chromium white irons. *Wear* **2015**, *332*, 1006–1011. [CrossRef]
10.   Gonzalez-Pocino, A.; Alvarez-Antolin, F.; Asensio-Lozano, J. Optimization, by Means of a Design of Experiments, of Heat Processes to Increase the Erosive Wear Resistance of White Hypoeutectic Cast Irons Alloyed with Cr and Mo. *Metals* **2019**, *9*, 403. [CrossRef]
11.   Guitar, M.A.; Nayak, U.P.; Britz, D.; Mucklich, F. The Effect of Thermal Processing and Chemical Composition on Secondary Carbide Precipitation and Hardness in High-Chromium Cast Irons. *Int. J. Met.* **2020**, *14*, 755–765. [CrossRef]
12.   Yang, H.S.; Wang, J.; Shen, B.L.; Liu, H.H.; Gao, S.J.; Huang, S.J. Effect of cryogenic treatment on the matrix structure and abrasion resistance of white cast iron subjected to destabilization treatment. *Wear* **2006**, *261*, 1150–1154. [CrossRef]
13.   Gonzalez-Pocino, A.; Alvarez-Antolin, F.; Asensio-Lozano, J.; Alvarez-Perez, H. Influence of Thermal Processing Factors, Linked to the Destabilisation of Austenite, on the Microstructural Variation of a White Cast Iron Containing 25% Cr and 0.6% Mo. *Metals* **2020**, *10*, 832. [CrossRef]
14.   Antolin, J.F.A.; Garrote, L.F.; Lozano, J.A. Application of Rietveld Refinement to the correlation of the microstructure evolution of white cast irons with 18 and 25 %-wt. Cr after oil quench and successive temper treatments, with abrasive wear and bending testing. *Revista de Metalurgia* **2018**, *54*, 11. [CrossRef]
15.   Pero-Sanz, J.A. *Aceros*; Dossat, Ed.; Dossat: Madrid, Spain, 2004; p. 558.
16.   Selte, A.; Ozkal, B.; Arslan, K.; Ulker, S.; Hatman, A. Effect of Nitriding on the Wear Resistance of Tool Powder Steels with Different Contents of V, Cr and Mo. *Met. Sci. Heat Treat.* **2018**, *59*, 729–734. [CrossRef]
17.   Binder, C.; Bendo, T.; Hammes, G.; Klein, A.N.; de Mello, J.D.B. Effect of nature of nitride phases on sliding wear of plasma nitrided sintered iron. *Wear* **2015**, *332*, 995–1005. [CrossRef]
18.   Gonzalez-Pocino, A.; Alvarez-Antolin, F.; Asensio-Lozano, J. Improvement of Adhesive Wear Behavior by Variable Heat Treatment of a Tool Steel for Sheet Metal Forming. *Materials* **2019**, *12*, 2831. [CrossRef]
19.   Garzon, C.M.; Franco, A.R.; Tschiptschin, A.P. Thermodynamic Analysis of M7C3 Carbide Dissolution during Plasma Nitriding of an AISI D2 Tool Steel. *ISIJ Int.* **2017**, *57*, 737–745. [CrossRef]
20.   Kallel, M.; Zouch, F.; Antar, Z.; Bahri, A.; Elleuch, K. Hammer premature wear in mineral crushing process. *Tribol. Int.* **2017**, *115*, 493–505. [CrossRef]
21.   Al-Bukhaiti, M.A.; Abouel-Kasem, A.; Emara, K.M.; Ahmed, S.M. A Study on Slurry Erosion Behavior of High Chromium White Cast Iron. *J. Tribol. Trans. ASME* **2017**, *139*. [CrossRef]
22.   Atapek, S.H.; Fidan, S. Solid-particle erosion behavior of cast alloys used in the mining industry. *Int. J. Miner. Metall. Mater.* **2015**, *22*, 1283–1292. [CrossRef]
23.   Prat-Bartés, A.; Tort-Martorell, X.; Grima-Cintas, P.; Pozueta-Fernández, L.; Solé-Vidal, I. *Métodos Estadísticos*, 2nd ed.; UPC: Barcelona, Spain, 2004; p. 376.